

PUBLISHED VERSION

P. Edward Purdue, Tania N. Crotti, Zhenxin Shen, Jennifer Swantek, Jun Li, Jonathan Hill, Adedayo Hanidu, Janice Dimock, Gerald Nabozny, Steven R. Goldring, Kevin P. McHugh
Comprehensive profiling analysis of actively resorbing osteoclasts identifies critical signaling pathways regulated by bone substrate

Scientific Reports, 2014; 4:7595-1-7595-11

This work is licensed under a Creative Commons Attribution-NonCommercial-NoDerivs 4.0 International License. The images or other third party material in this article are included in the article's Creative Commons license, unless indicated otherwise in the credit line; if the material is not included under the Creative Commons license, users will need to obtain permission from the license holder in order to reproduce the material. To view a copy of this license, visit <http://creativecommons.org/licenses/by-nc-nd/4.0/>

PERMISSIONS

<http://creativecommons.org/licenses/by-nc-nd/4.0/>



Attribution-NonCommercial-NoDerivatives 4.0 International (CC BY-NC-ND 4.0)

This is a human-readable summary of (and not a substitute for) the [license](#)

[Disclaimer](#)

You are free to:

Share — copy and redistribute the material in any medium or format

The licensor cannot revoke these freedoms as long as you follow the license terms.

Under the following terms:



Attribution — You must give [appropriate credit](#), provide a link to the license, and [indicate if changes were made](#). You may do so in any reasonable manner, but not in any way that suggests the licensor endorses you or your use.



NonCommercial — You may not use the material for [commercial purposes](#).



NoDerivatives — If you [remix, transform, or build upon](#) the material, you may not distribute the modified material.

No additional restrictions — You may not apply legal terms or [technological measures](#) that legally restrict others from doing anything the license permits.

8 September, 2015

<http://hdl.handle.net/2440/94187>



OPEN

SUBJECT AREAS:

EXTRACELLULAR
SIGNALLING MOLECULES
TRANSCRIPTOMICSReceived
8 October 2014Accepted
2 December 2014Published
23 December 2014

Correspondence and requests for materials should be addressed to P.E.P. (purduee@hss.edu) or K.P.M. (kmchugh@dental.ufl.edu)

Comprehensive profiling analysis of actively resorbing osteoclasts identifies critical signaling pathways regulated by bone substrate

P. Edward Purdue¹, Tania N. Crotti^{2,3}, Zhenxin Shen³, Jennifer Swantek⁴, Jun Li⁴, Jonathan Hill⁴, Adedayo Hanidu⁴, Janice Dimock⁴, Gerald Nabozny⁴, Steven R. Goldring¹ & Kevin P. McHugh⁵

¹Hospital for Special Surgery, New York, NY 10021, ²School of Medical Sciences, The University of Adelaide, Adelaide 5005, Australia, ³Beth Israel Deaconess Medical Center, Boston, MA 02215, ⁴Boehringer Ingelheim Pharmaceuticals Inc., Ridgefield, CT, 06877, ⁵University of Florida College of Dentistry, Gainesville, FL, 32610.

As the only cells capable of efficiently resorbing bone, osteoclasts are central mediators of both normal bone remodeling and pathologies associates with excessive bone resorption. However, despite the clear evidence of interplay between osteoclasts and the bone surface *in vivo*, the role of the bone substrate in regulating osteoclast differentiation and activation at a molecular level has not been fully defined. Here, we present the first comprehensive expression profiles of osteoclasts differentiated on authentic resorbable bone substrates. This analysis has identified numerous critical pathways coordinately regulated by osteoclastogenic cytokines and bone substrate, including the transition from proliferation to differentiation, and sphingosine-1-phosphate signaling. Whilst, as expected, much of this program is dependent upon integrin beta 3, the pre-eminent mediator of osteoclast-bone interaction, a surprisingly significant portion of the bone substrate regulated expression signature is independent of this receptor. Together, these findings identify an important hitherto underappreciated role for bone substrate in osteoclastogenesis.

The function of osteoclasts is to resorb bone, and they represent the major cell type responsible for this critical step in homeostatic bone remodeling and in pathological bone loss disorders^{1,2}. Recent years have seen remarkable advances in the understanding of the signaling pathways required for osteoclast formation and activation, and of how these processes are regulated by the essential osteoclastogenic cytokines Receptor activator of nuclear factor kappa-B ligand (RANKL) and Macrophage colony-stimulating factor (M-CSF)^{3–5}. RANKL and M-CSF are necessary and sufficient for the *in vitro* generation from myeloid precursor cells of multinucleated cells that bear the hallmarks of osteoclasts. The ability to generate osteoclast-like cells *in vitro* with high efficiency has been instrumental in identifying at a molecular level numerous key factors involved in this process. However, these studies have almost without exception been limited to cells differentiated on tissue culture plastic or glass surfaces, and have therefore failed to address the critical role played by bone substrate in osteoclast differentiation, polarization, and activation^{6–11}. Since fully functional osteoclasts exist exclusively upon bone surfaces *in vivo*, the paucity of information regarding how bone substrate regulates these cells represents a significant and important gap in our knowledge of osteoclast biology.

Integrin beta 3 (itgb3) is a critical mediator of the interaction of differentiating osteoclasts with bone substrate^{12,13}. Itgb3 is highly induced in differentiating and mature osteoclasts, and forms a complex with integrin alpha v on the surface of osteoclasts that binds to extracellular matrix components present in bone and thus plays an important role in osteoclast-bone interactions. Mice lacking itgb3 generate osteoclasts that are unable to properly polarize upon bone substrates, and thus exhibit a defect in bone resorption, accentuating the critical role of itgb3 mediated adhesion to bone in osteoclast differentiation and activation¹². A critical role for itgb3 has also been demonstrated in mouse models of ovariectomy-induced osteoporosis¹⁴ and cancer metastasis to bone¹⁵.

In this study we have provided the first comprehensive gene expression profiling of mouse bone marrow macrophage (BMM)-derived osteoclasts on bone and hydroxyapatite (HA) substrates. Using time course analysis of osteoclasts generated on plastic, HA and bone, we have identified a unique cluster of osteoclast genes specifically up-regulated by bone substrate. Further, we have compared the induction of these genes in wild type and



itgb3 knockout (*Itgb3* $-/-$) cells differentiated on bone to delineate the role of itgb3 in activation of bone-dependent osteoclast genetic programs. These analyses identified the pathway responsible for synthesis, transport and signaling by the lipid mediator sphingosine-1-phosphate (S-1-P) as a prototypical member of the bone- and itgb3-regulated genes and additional studies confirmed the critical role of this pathway in regulating the differentiation and activation of osteoclasts. Furthermore, we have demonstrated that bone substrate regulates the switch from cell cycle progression to differentiation and activation at late stages of osteoclastogenesis.

Results

Expression profiling of mouse osteoclasts differentiated on bone related substrates. In order to determine the role of bone matrix in osteoclast formation and function, we differentiated mouse BMMs to osteoclasts on authentic devitalized mouse bone, or on the non-bone substrates HA or tissue culture plastic. After 5 days of culture with RANKL, osteoclasts on mouse calvarial bone discs displayed actin rings characteristic of polarized and actively resorbing osteoclasts while osteoclast-like cells on plastic displayed characteristic podosome bands (Fig. 1a and 1b respectively)¹⁶.

As detailed in *Methods*, quadruplicate cultures prepared from individual animals were processed for RNA extraction at early (day 1), intermediate (day 3) and terminal (day 5) stages of RANKL-induced osteoclastogenesis. BMMs were cultured for equivalent times on mouse bone, HA and tissue culture plastic, in the presence of M-CSF, but not RANKL as a control.

Following confirmation of RNA quality by Biacore analysis and analysis of results from hybridization to test chips, genome-wide expression profiles were determined on Affymetrix Gene Chips (Mouse Genome 430 2.0) for each of the 4 replicates with and without RANKL, on each substrate and over 3 time points. Hierarchical cluster analysis identified gene clusters specifically regulated by RANKL (independent of substrate) and by substrate-dependence (Fig. 1c). In accordance with previous studies, this analysis revealed that RANKL, independent of substrate, induced expression of subsets of genes with known involvement in osteoclast biology and function, including: TRAP, cathepsin-k, calcitonin receptor, itgb3, OSCAR, and NFATc1. The RANKL-induced expression profiles transitioned substantially during the time-course of the analysis, as the macrophage precursors differentiated through the stages of pre-osteoclast, committed osteoclast precursors, and differentiated, bone-resorbing osteoclast. As delineated in Fig. 1d, the number of RANKL regulated genes increased substantially between days 1–3, when pre-osteoclasts are differentiating into immature osteoclasts, and increased more moderately during the later stages of differentiation of fully mature osteoclasts (days 3–5).

Substrate induction of RANKL induced genes. Notably, we also observed that the well-established pattern of RANKL-induced osteoclast gene expression could be significantly reprogrammed by the nature of the growth substrate. At each time point, a subset of the RANKL-induced genes was further regulated by the presence of bone. Osteoclasts differentiated on HA substrate (not shown) tended towards an expression profile intermediate to those seen on plastic and bone. As shown in Fig. 1d, the numbers of RANKL-induced genes that were super-regulated both positively and negatively by bone substrate, were considerably higher on day 5, when the osteoclasts are undergoing terminal differentiation and activation, than at earlier time points. Interestingly, there was little overlap in the gene sets super-regulated by bone at the different time-points (Fig. 1e), suggesting that the bone regulated expression program is linear and highly dynamic, and dependent upon the differentiation state of the cell.

Specific subsets of bone-regulated osteoclast genes are dependent upon itgb3, whereas other genes are itgb3-independent. Since itgb3 has been shown to play a critical role in regulating the morphological and functional activity of osteoclasts¹², we next assessed the contribution of itgb3 signaling to the identified bone-dependent gene expression profile. Consistent with its role in interaction with bone substrate, expression of itgb3 was induced by RANKL, and super-induced by bone substrate during late stages of osteoclast differentiation (Fig. 2a). To directly address the role of itgb3 in bone regulated osteoclastogenesis, BMMs from three individual wild-type and three individual *Itgb3* knockout mice (*Itgb3* $-/-$) were isolated and subjected to osteoclastogenesis (in the presence of M-CSF and RANKL) on tissue culture plastic and devitalized mouse calvarial bone slices, as described above. Actin ring staining by Rhodamine Phalloidin confirmed that although *itgb3* $-/-$ osteoclasts retain the ability to attach to the bone surface, they fail to form actin rings, consistent with the defective resorption activity of osteoclasts lacking itgb3 (Fig. 2b)^{12,17–22}.

Consistent with the pre-eminent role of itgb3 in osteoclastogenesis, microarray analysis and hierarchical clustering (Fig. 2c) revealed that absence of this integrin resulted in significant changes in the pattern of gene expression during RANKL-induced differentiation of BMMs. Significantly, cluster analysis identified not only sets of bone-regulated genes that were dependent upon the presence of itgb3, but a novel cluster of genes whose induction by bone substrate was unaffected or enhanced by the absence of itgb3. The identification of bone-regulated, itgb3-independent genes is notable since it implies the existence of multiple bone-derived signaling pathways for regulation of gene expression in differentiating osteoclasts.

Independently qPCR analysis was utilized to confirm the ability of bone to up-regulate specific osteoclast genes in either an itgb3-independent (e.g. AnxA8) or itgb3-dependent (e.g. UCHL1 and FKBp9) manner (Table 1).

Taken together, the results from expression profiling show that multiple mechanisms including cytokine signaling (RANKL), integrin-based attachment to substrate (itgb3) and the nature of the substrate itself (bone) drive gene expression and cell differentiation of osteoclasts. Moreover, these different regulators of osteoclast differentiation operate in overlapping fashion to coordinate the complex events that constitute osteoclast formation and activation.

Pathway analysis and functional classification. Several approaches were taken towards identification of the signaling pathways coordinately regulated by bone substrate and/or itgb3 during RANKL-induced osteoclastogenesis. Ingenuity Pathway Analysis (IPA) identified several bone regulated functional categories, including regulation of cell survival and proliferation (Table 2). Gene Set Enrichment Analysis (GSEA) was further used as a means to look for pathways that were differentially regulated by these stimuli. This confirmed that bone substrate profoundly influences osteoclast proliferation and differentiation, as highlighted by a bone substrate-induced repression of expression of genes associated with cell cycle progression and cell division (Fig. 3a).

As highlighted for representative genes cdc7 and cyclin b1 (Fig. 3b), genes within this pathway show a modest decrease between days 3–5 on plastic, but a much more prominent loss of expression during the same period of culture on bone. The repression of cell cycle genes in osteoclast differentiation on bone indicates the induction of a transcriptional program that arrests osteoclast proliferation during the late stages of osteoclast differentiation. Absence of itgb3 had a remarkably similar impact upon this pathway as absence of bone (i.e. growth on plastic), with numerous genes associated with cell cycle progression being elevated in day 5 osteoclasts in the absence of itgb3 (Fig. 3a). This strongly reaffirms the importance of itgb3 for osteoclast development, and indicates that the bone

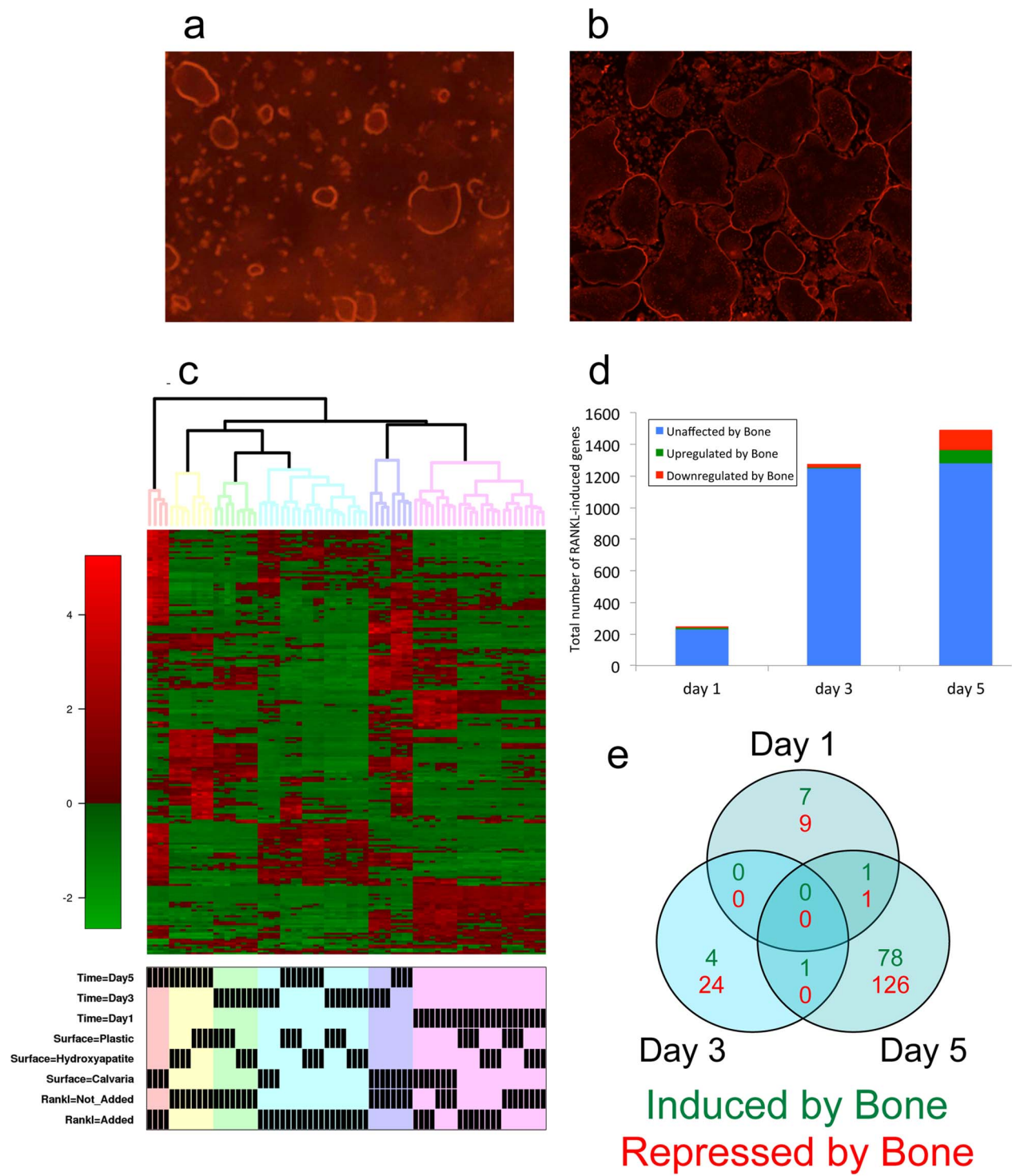


Figure 1 | Bone substrate regulates gene expression in differentiating murine osteoclasts. (a) Phalloidin stain showing distinctive actin morphology of wild type BMM-derived osteoclasts differentiated on bone. (b) Phalloidin stain showing distinctive actin morphology of wild type BMM-derived osteoclasts differentiated on plastic. (c) Hierarchical clustering heat map of mouse BMM-derived osteoclast expression profiles regulated by RANKL, stage of differentiation and culture substrate. (d) Total numbers of RANKL-induced genes that are further regulated, or unaffected, by bone substrate. (e) Venn diagram of the overlap between genes regulated $>2\times$ by bone on days 1, 3 and 5.

substrate mediated decline in cell cycle progression is a highly itgb3-dependent process. Interestingly, macrophages cultured in the absence of RANKL also show a decrease in expression of cdc7 and Cyclin B1 between 3 and 5 days in culture (–RL in Fig. 3b) as the cells reach confluence. However, unlike in osteoclasts, this effect is not modulated by bone substrate, suggesting that the bone substrate-mediated switch from proliferation to activation is specific for

RANKL-induced osteoclasts and not a common feature of myeloid cells.

Regulation of the S-1-P pathway during osteoclastogenesis on bone substrate. GSEA analysis identified several additional pathways regulated by bone and itgb3. Prominent among these was the S-1-P pathway (termed the EDG1 pathway in this analysis,

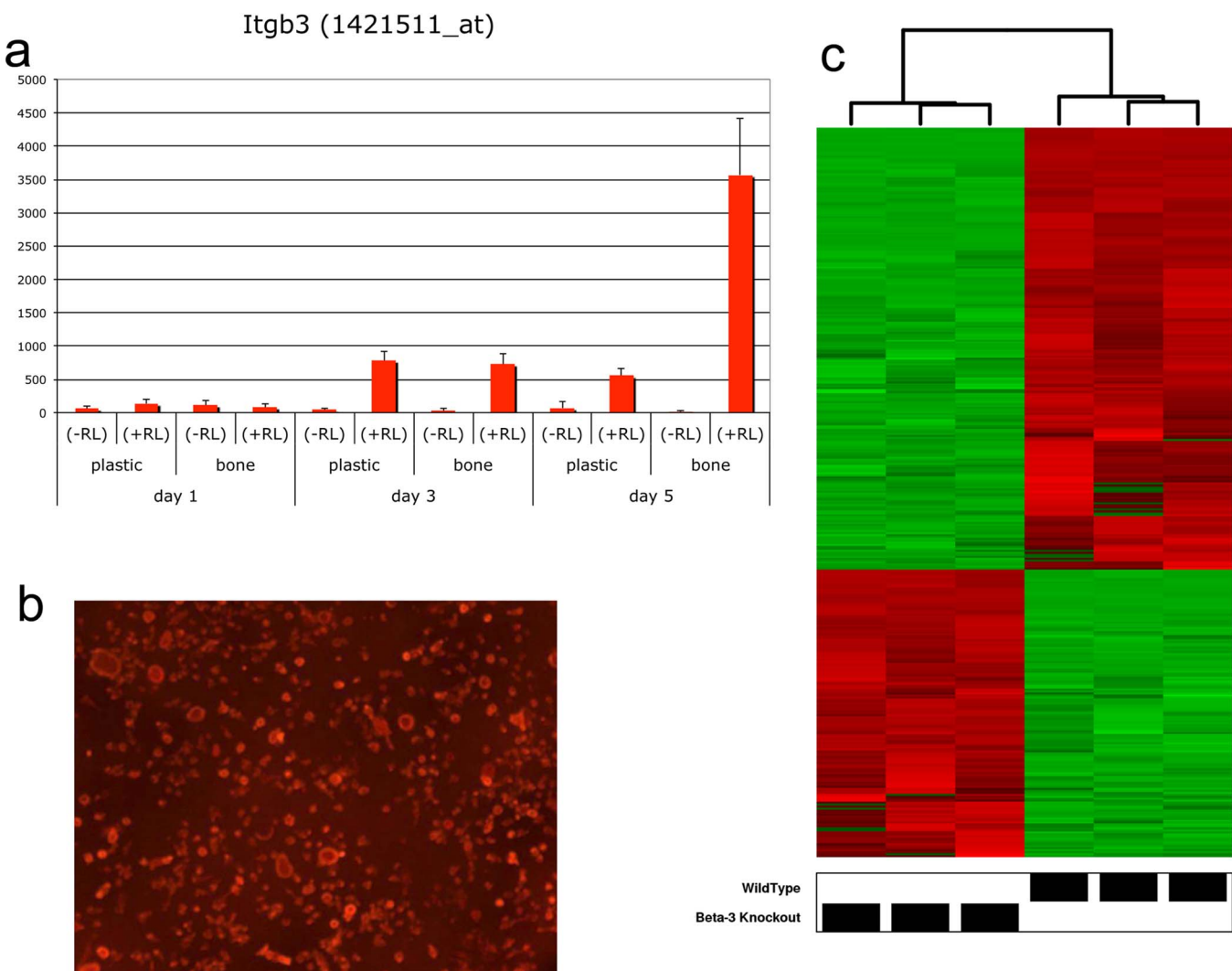


Figure 2 | Itgb3 signaling mediates the effects of bone substrate on osteoclastogenesis. (a) Detailed microarray analysis of *itgb3* expression in cells cultured for 1, 3 and 5 days on plastic or calvaria (bone), in the presence (+ RL) or absence (− RL) of RANKL. (b) Phalloidin stain showing distinctive actin morphology of *itgb3* deficient BMM-derived osteoclasts differentiated on bone. (c) Hierarchical clustering heat map of mouse BMM-derived bone induced osteoclast expression profiles regulated by *itgb3*.

with EDG1 being a cell surface receptor for S-1-P), which includes the protein mediators involved in the generation, transport and signaling of S-1-P. Based upon this observation, and the fact that a number of reports have suggested an important role for S-1-P and

EDG signaling in osteoclast biology^{23–28}, we investigated this pathway in greater detail.

GSEA analysis revealed that the S-1-P pathway was significantly regulated independently by RANKL, bone substrate and *itgb3*

Table 1 | Comparison of microarray and quantitative RT-PCR expression analysis for selected genes. Wild-type (WT) and integrin beta 3 deficient (*Itgb3KO*) cells were cultured on plastic or bone substrate with M-CSF and RANKL for 5 days. For each analysis, expression in wild-type cells (WT) cultured on plastic is set to a value of 1.00, and relative values and standard deviations calculated. Primer sequences are given in the Methods Section

Gene	Microarray Analysis				Quantitative RT-PCR			
	WT Plastic	WT Bone	<i>Itgb3KO</i> Plastic	<i>Itgb3KO</i> Bone	WT Plastic	WT Bone	<i>Itgb3KO</i> Plastic	<i>Itgb3KO</i> Bone
AnxA8 (1425789_s_at)	1.00 (0.60)	12.86 (0.80)	0.46 (0.28)	13.33 (1.98)	1.00 (.034)	66.47 (16.98)	1.34 (0.04)	73.96 (19.40)
AnxA8 (1417732_at)	1.00 (0.33)	14.40 (0.80)	0.64 (0.23)	15.88 (1.87)				
UCHL1 (1448260_at)	1.00 (0.04)	1.69 (0.06)	0.02 (0.005)	0.04 (0.01)	1.00 (0.13)	2.09 (0.34)	0.02 (0.01)	0.06 (0.03)
FKBP9 (1423677_at)	1.00 (0.08)	1.58 (0.12)	0.19 (0.04)	0.16 (0.04)	1.00 (0.41)	2.91 (1.23)	0.20 (0.09)	0.21 (0.19)
FKBP9 (1437687_x_at)	1.00 (0.02)	1.49 (0.03)	0.15 (0.002)	0.13 (0.01)				
SphK1 (1451596_a_at)	1.00 (0.03)	1.52 (0.16)	0.60 (0.06)	0.80 (0.08)	1.00 (0.66)	1.54 (0.48)	0.57 (0.15)	0.83 (0.51)
Spns2 (1451601_a_at)	1.00 (0.09)	1.69 (0.07)	1.62 (0.08)	1.48 (0.21)	1.00 (0.26)	2.39 (0.41)	1.51 (0.70)	1.76 (0.39)

**Table 2 | Pathway and functional analysis of gene sets regulated by bone substrate**

Category	p-Value	Molecules
Cellular Function and Maintenance	4.65E-06	ACAP1, ATG4C, ATM, AXL, BNIP3, CA9, CADM1, CADPS, CCL22, CLEC6A, COL5A3, CRYAB, CXCL3, DCLRE1C, DDIT4, EGR1, ERO1L, FAS, FCGR2B, FPR2, FXYD2, GATM, GHR, GNA13, ICA1, IL7R, KCNJ10, KIF5B, LAMA3, MAP1LC3A, MBP, MED1, MSR1, MT1H, MTM1, MYSM1, NDRG1, NMB, NOS3, NPY, NUCB2, NUPR1, Rps6/Rps6-ps4, SESN2, SLC12A2, SLC2A1, SLC37A4, SLC8A1, STAP2, TRIB3, WWP2, ZEB1
Cell Death and Survival	1.25E-05	ABCA3, AIM2, ALDH2, AMACR, AQP9, ARG1, ATM, AXL, BMP2, BNIP3, BUB1, CA9, CADM1, CADPS, CASP4, CCL27, CD2AP, CD300LD, Cd59a, CHST11, COL5A3, CRYAB, CTH, CXCL3, DCLRE1C, DDIT4, DSG2, DSP, EGR1, EHD3, EYA1, FAM162A, FAS, FCGR2B, FHL2, FOXK2, FSTL1, FUBP1, G2E3, GHR, GLO1, GNA13, GNAI1, GRIA3, H60a, HK2, HYOU1, IBSP, Ifi202b, IL7R, ITCH, ITGB3, JAG1, KCNJ10, KLRD1, LAMA3, LAT51, MAP1LC3A, MBD4, MBP, MED1, MPO, MSI2, MSR1, MT1H, MTM1, NDRG1, NLE1, NOS3, NPY, NSF, NUPR1, PAFAH1B2, POU2AF1, PPP2R1B, Pvr, RAI14, Rps6/Rps6-ps4, SESN2, SIK1, SLC12A2, SLC2A1, SLC8A1, STAP2, SUB1, TIA1, TIMP2, TNFRSF14, TNFRSF9, TRIB3, UCHL1, URI1, VAMP3, WASF1, WWP2, XAF1, ZEB1, ZFR
Cellular Growth and Proliferation	1.81E-05	ADAMTS4, AIM2, AK4, AMACR, APOBEC1, AQP9, ARF1, ARG1, ARHGAP5, ARHGDIG, ATM, AXL, BMP2, BNIP3, BPNT1, BUB1, CA9, CACUL1, CADM1, CCDC19, CCL27, CD2AP, Cd59a, CD84, CHST11, CREB3, CRYAB, CTH, CXCL3, DCLRE1C, DFNA5, DSG2, DSP, DUSP8, EGR1, ELOVL7, EPS8, ERO1L, EYA1, FAS, FCGR2B, FHL2, FPR2, FSCN1, FXYD2, GFER, GHR, GNA13, GNAI1, GRIA3, H60a, HAO1, HK2, IBSP, Ifi202b, Ifi204, IGF2BP3, IL7R, ITCH, ITGB3, JAG1, KLRD1, LAMA3, LAT51, MAPRE1, MBP, MED1, MSI2, MSR1, MT1H, NDRG1, NMB, NOS3, NPY, NUCB2, NUPR1, P4HA2, PLS3, POU2AF1, PPP2R1B, PTX3, Pvr, QPCT, RHOU, SIK1, SLC12A2, SLC2A1, SLC8A1, STAP2, TIMP2, TLE6, Tmsb4x, TNFRSF14, TNFRSF9, TPM2, TRIB3, UCHL1, URI1, VLDR, VPS39, WLS, WWP2, ZEB1
Cellular Movement	2.21E-05	AQP9, ARF1, ARG1, ARHGAP5, ATM, AXL, BMP2, C1GALT1, CA9, CADM1, CCL22, CCL27, Cd59a, CD99L2, CREB3, CRYAB, CXCL3, EGR1, ELK3, EPS8, FAS, FCGR2B, FHL2, FPR2, FSCN1, FSTL1, GNA13, GNAI1, GRIA3, ITCH, ITGB3, JAG1, LAMA3, MAPRE1, MBP, MED1, MPO, MSR1, NDRG1, NOS3, NPY, NUCB2, P4HA2, POU2AF1, PTX3, Pvr, QPCT, RAP2B, RHOU, ROPN1L, SEMA3C, SLC12A2, SLC2A1, SLC37A4, SLC8A1, STAP2, TIMP2, TLE6, Tmsb4x, TNFRSF14, TNFRSF9, USP14, VLDR, WASF1, ZEB1
Amino Acid Metabolism	2.47E-05	GATM, NAGS, NOS3, QPCT

(Fig. 4a). Analysis of the microarray data for probes for sphingosine kinase 1 (SphK1), a key regulator of S-1-P synthesis, revealed robust induction by RANKL during osteoclast differentiation (day 3–5), with super-induction by bone substrate most prominent at later stages of terminal differentiation and activation (day 5) (Fig. 4b), whereas the related kinase SphK2 was not regulated by RANKL or bone substrate (not shown). Interestingly, Spns2, a more recently identified S-1-P transporter²⁹, is regulated in a manner very similar to that of SphK1, suggesting coordinated regulation of S-1-P synthesis and transport (Fig. 4b). Pathway analysis revealed that key components of the S-1-P pathway are regulated by each of the critical determinants of osteoclast formation and activation; RANKL, bone and itgb3 (Fig. 4c), suggesting that this pathway integrates signals emanating from RANKL signaling, itgb3 engagement, and attachment to bone. Finally, immunohistochemical analysis of bone erosions in tissue from a patient with rheumatoid arthritis (RA) revealed strong and specific SphK1 expression within osteoclasts indicating that the initial observation of SphK1 up-regulation in bone adherent osteoclasts using mouse cells in culture is directly translated to human osteoclasts associated with inflammatory bone loss (Fig. 4d). Additionally, attachment of these osteoclasts to the bone surface further supports the SphK1 kinase as a target of regulation by bone.

SphK1 inhibitors negatively regulate osteoclastogenesis. The preceding results show that the S-1-P pathway is up-regulated in response to RANKL and also to bone substrate, and that this up-regulation is dependent, at least in part, by itgb3-mediated interactions between the differentiating osteoclasts and the bone substrate. To address the role of EDG pathway induction in osteoclastogenesis, SphK inhibitors N',N' Dimethylsphingosine (N',N'-DMS) and the SphK1-selective Compound 54³⁰ were evaluated for effects on *in vitro* osteoclast formation from human and mouse precursors.

To assess the potential effects of SphK1 inhibition on osteoclastogenesis, mouse BMM were incubated with M-CSF and RANKL in the presence or absence of different doses of the SphK inhibitors. When

present throughout the 5 days of culture, both inhibitors dose-dependently inhibited generation of tartrate resistant acid phosphatase (TRAP)-positive multinuclear osteoclasts (Fig. 5a). As expected, loss of formation of TRAP-positive osteoclasts was reflected in an inhibition in the formation of resorptive pits when the osteoclasts were generated on bone slices (Fig. 5b). In addition, induction of expression of osteoclast specific genes was also dose-dependently inhibited by both of the inhibitors, as illustrated for cathepsin K (Fig. 5c). To address at which stage of osteoclastogenesis SphK1 activity is required, osteoclastogenesis assays were performed in which inhibitors were only present during either the first 3 days of culture, or the final 2 days. Interestingly, inhibition of osteoclastogenesis was seen in both cases, albeit to a lesser degree than when inhibitors were present throughout, suggesting that SphK1 inhibition can block osteoclast formation at multiple stages of differentiation (Fig. 5a). Finally, the effects of SphK1 inhibitors on human monocyte-derived osteoclastogenesis were evaluated. As seen for murine cells, these validated inhibitors showed a dose dependent inhibition of RANKL-induced formation of TRAP-positive osteoclasts (Fig. 5d) as well as inhibition of osteoclast gene expression (data not shown). These results show that SphK1 inhibition potently blocks induction of osteoclast genes and formation of multinucleated osteoclasts in both mouse and human *in vitro* systems.

Taken together, these results show that genes of the S-1-P pathway are not only co-coordinately regulated by RANKL signaling, itgb3-mediated attachment, and bone substrate, but also that this pathway plays a critical role in osteoclastogenesis and activation. In turn, this validates the profiling studies on the role of bone and itgb3 for the identification of important pathways regulating osteoclastogenesis on bone substrates.

Discussion

By definition, functional osteoclasts exist only on bone surfaces, both in the context of normal bone homeostasis and in inflammatory

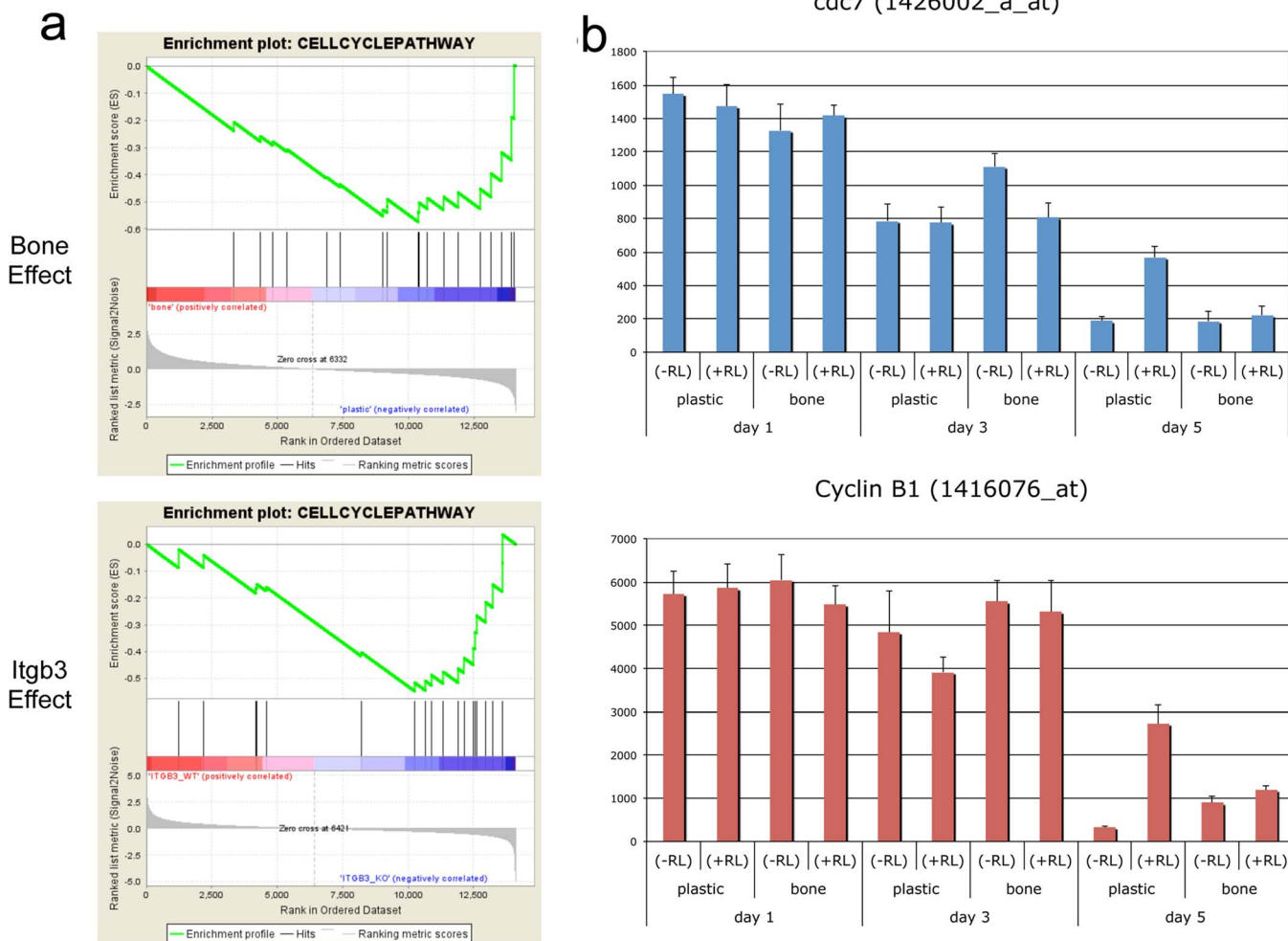


Figure 3 | Regulation of cell cycle progression and proliferation by bone substrate and itgb3. (a) GSEA analysis showing modulation of the cell cycle progression pathway by both bone and itgb3. (b) Detailed microarray analysis of cdc7 and Cyclin B1 probe sets in cells cultured for 1, 3 and 5 days on plastic or calvaria (bone), in the presence (+RL) or absence (-RL) of RANKL.

osteolysis, since it is only when associated with bone that these cells perform their unique and required cellular activity, namely bone resorption. This observation stresses the importance of considering the cell culture substrate when analyzing the cellular and molecular mechanisms regulating osteoclast differentiation and activation *in vitro*. To address this need, we have recently demonstrated that differentiation on bone substrates can profoundly influence osteoclast differentiation^{8,9,11}. A wealth of valuable information on the regulation of osteoclastogenesis has been derived from studies of osteoclast cells on tissue culture plastic induced by the pro-osteoclastogenic cytokines M-CSF and RANKL^{6,7,31–37}. However, little attention has been paid to this process in the context of bone substrate, leaving the details of bone regulation of osteoclast gene expression largely unexplored. This remains an important gap in our knowledge of osteoclast biology, particularly so because bone regulated osteoclast products may represent novel and specific candidate molecules for therapeutic targeting of the osteoclast. In this paper, we have addressed this knowledge gap by providing the first comprehensive characterization on the role of bone substrates on gene expression during osteoclast differentiation and activation.

Microarray analysis, coupled to qPCR validation and pathway analysis revealed a number of gene clusters specifically modified by bone substrate. Focusing on bone regulation of gene sets induced by RANKL identified coordinated repression by bone during the later stages of osteoclastogenesis of genes involved in cell cycle pro-

gression and cell division. This would be consistent with a transition during late osteoclastogenesis from expansion and fusion of the precursor pool towards polarization and initiation of bone resorption (a process that can not occur on tissue culture plastic). Although earlier studies^{38–40} reported that RANKL can induce downregulation of cell cycle progression genes during the late stages of osteoclast differentiation, these studies were limited to cells cultured on plastic. Our results indicate that signaling mediated by bone substrate and itgb3 plays a crucial role in the life cycle of the osteoclast by regulating the switch from proliferation to terminal differentiation and activation of bone resorption. It is interesting to note that the bone substrate mediated repression of expression of genes associated with cell cycle progression in developing osteoclasts is not seen in macrophages differentiated in the absence of RANKL. Macrophages, like osteoclasts, show a decrease in expression of cell cycle progression genes during extended culture, likely reflecting a transition to confluence. Importantly, however, unlike the bone substrate-mediated switch from osteoclast proliferation to activation, macrophage cell cycle progression is not further regulated by bone substrate.

In addition to the observed effect on regulation of cell cycle progression and cell division, bone substrate was also shown to significantly regulate the S-1-P pathway responsible for the biosynthesis, transport and signaling of S-1-P. Moreover, this pathway was independently regulated by RANKL signaling, bone substrate and itgb3 mediated attachment of osteoclasts to bone, indicating that multiple

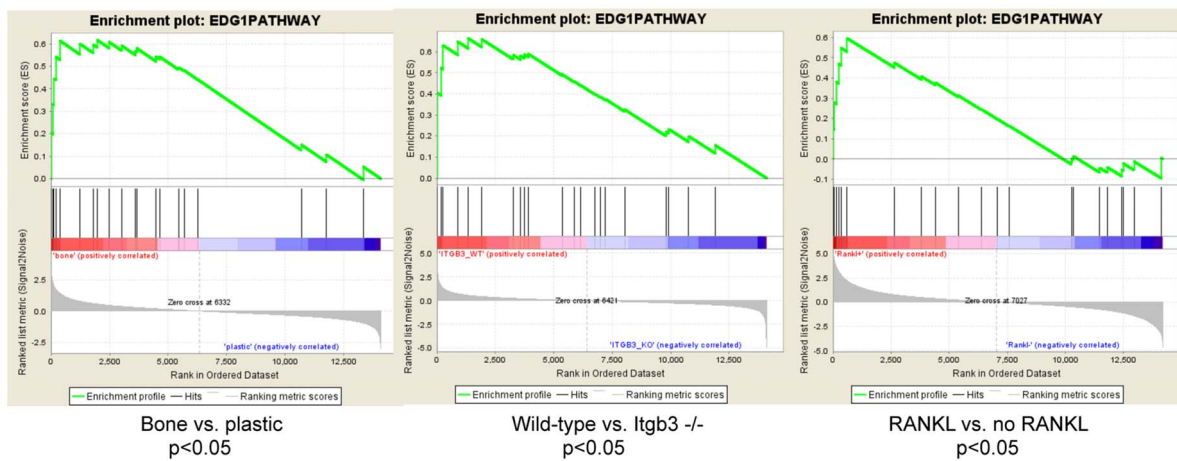
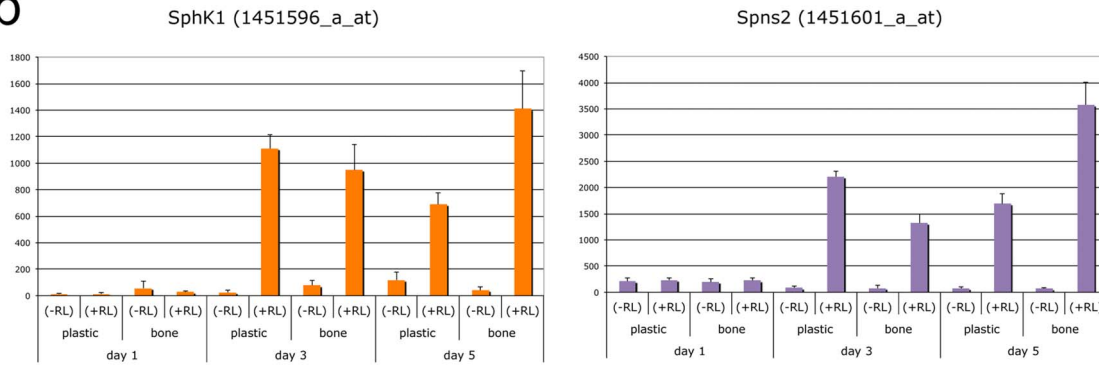
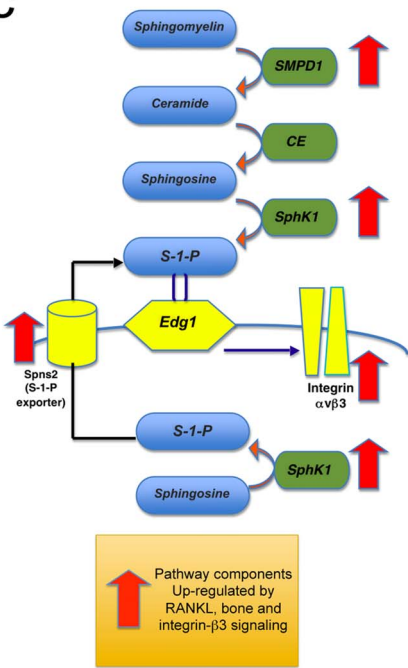
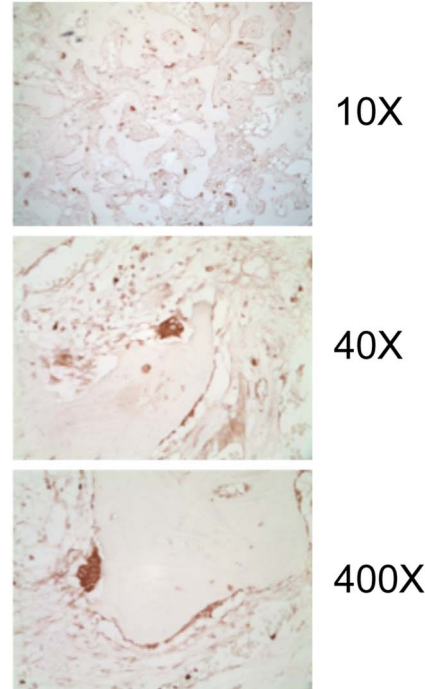
**a****b****c****d**

Figure 4 | Regulation of the S-1-P pathway by RANKL, bone and itgb3. (a) GSEA analysis showing that RANKL, bone and itgb3 each independently modulates this pathway. (b) Detailed microarray analysis of SphK1 and Spns2 probe sets in cells cultured for 1, 3 and 5 days on plastic or calvaria (bone), in the presence (+RL) or absence (-RL) of RANKL. (c) Pathway analysis showing S-1-P pathway components that are co-coordinately regulated by RANKL, itgb3 and bone substrate during osteoclastogenesis. (d) Immunohistochemistry analysis showing SphK1 expression in osteoclasts on the bone surface in sites of rheumatoid arthritis bone erosions.

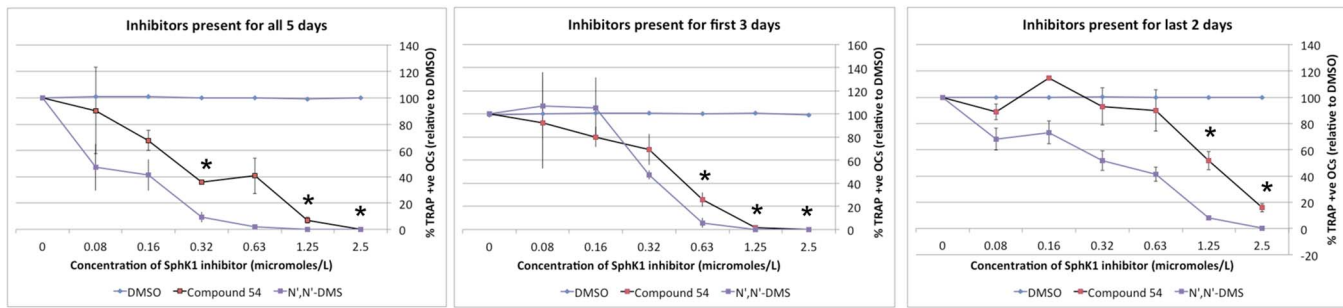
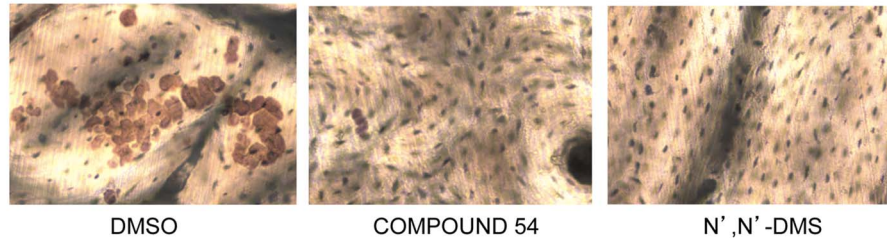
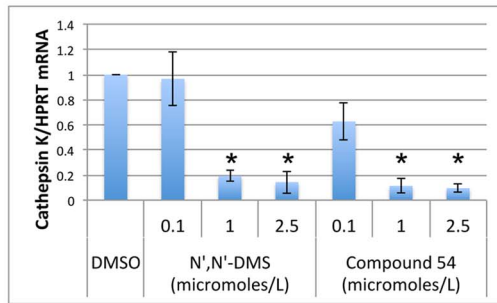
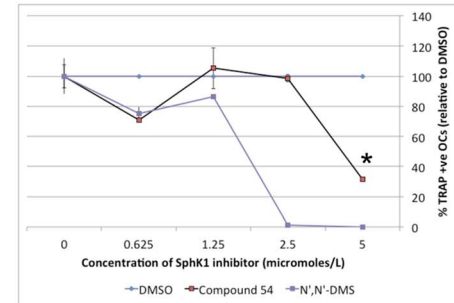
**a****b****c****d**

Figure 5 | Inhibition of SphK1 represses RANKL-induced murine and human osteoclastogenesis on plastic and bone. (a) Inhibition of RANKL-induced murine osteoclast formation by SphK1 inhibitors ($\text{N}'\text{,N}'\text{-DMS}$ and Compound 54) as assessed by quantitation of TRAP-positive multinucleated cells ($n = 3$, $* = p < 0.05$ compared to DMSO control). (b) Pit formation assay showing that the inhibitors (at $2.5 \mu\text{M}$) inhibit osteoclast mediated bone resorption. (c) Effects of SphK1 inhibitors on RANKL-induced expression of Cathepsin K as assessed by quantitative PCR ($n = 3$, $* = p < 0.05$ compared to DMSO control). (d) Inhibition of RANKL-induced human monocyte-derived osteoclast formation by SphK1 inhibitors ($\text{N}'\text{,N}'\text{-DMS}$ and Compound 54) as assessed by quantitation of TRAP-positive multinucleated cells (representative experiment of three).

signals driving osteoclast differentiation converge upon this pathway. We observe tight coupling between induction of sphingosine kinase (to generate S-1-P) and the transporter Spns2 (to export S-1-P), suggesting that upregulation of the S-1-P pathway during osteoclastogenesis is coupled to increased production and autocrine/paracrine signaling by S-1-P. Immunohistochemical analysis on samples from RA patients confirmed that SphK1 is strongly expressed in bone resorbing inflammatory osteoclasts in humans. Importantly, we demonstrated SphK1 inhibitors blocked *in vitro* differentiation of mouse and human osteoclasts and expression of osteoclast associated genes. Consistent with the inhibition of TRAP-positive osteoclast formation and osteoclast gene expression, SphK1 inhibition also eliminated bone resorption following osteoclast differentiation on bone substrate, although further studies are needed to determine whether this is secondary to differentiation defects, or indicative of a direct involvement of SphK1 in osteoclast activation. Such studies will focus on the effects on osteoclast resorptive activity of inhibiting SphK1 following terminal differentiation on bone substrates. Taken together, these results suggest that the S-1-P pathway is a critical mediator of osteoclastogenesis that is up-regulated not only by RANKL signaling, but also during later stages of osteoclast differentiation by Itgb3-mediated attachment to bone.

Sphingosine kinase and S-1-P signaling have previously been implicated in various aspects of osteoclast biology. Ishii et al.^{23–25} have

demonstrated that interactions between S-1-P and the S-1-P receptor S1PR1 on osteoclast precursors mediated chemotaxis of these cells to bone surfaces from the bloodstream, and hence regulate bone homeostasis. S1PR1 expression is down-regulated during RANKL-induced differentiation of osteoclast precursors (a finding confirmed by our microarray data). However, as previously described by Pederson et al.²⁷ and validated in the present study, differentiating osteoclasts greatly amplify their ability to generate S-1-P and hence potentially recruit additional precursors to the sites of fusion and osteoclast activation, as well as regulating coupling to bone formation via interaction with S-1-P receptors on the surface of osteoblasts. Our findings that inhibition of SphK1 represses not only generation of multinucleated osteoclasts but also expression of multiple early and late osteoclast genes suggests that the role of S-1-P in osteoclastogenesis is not limited to recruitment of precursors to fusing osteoclasts. This is further supported by the observation that inhibition of SphK1 during early (pre-fusion) stages of osteoclastogenesis is sufficient to block differentiation. It has been reported that one of the SphK inhibitors used here ($\text{N}'\text{,N}'\text{-DMS}$) represses osteoclastogenesis in a SphK1-independent manner⁴¹; however, our observation that Compound 54, a SphK1-specific inhibitor, blocks osteoclast formation argues against this. However, the mechanism(s) by which SphK1 generated S-1-P inhibits osteoclastogenesis remain to be elucidated. In addition to signaling through cell surface S-1-P receptors, S-1-P



can act intracellularly, raising the possibility of involvement of multiple possible paracrine and cell-autonomous mechanisms.

In addition to the above described roles of S-1-P signaling in RANKL-induced osteoclastogenesis, several lines of evidence point towards involvement of this pathway in the regulation of TNF signaling. SphK1 deficiency protects mice from TNF-induced arthritis⁴². Mechanistically, SphK1-generated S-1-P has been shown to act as a cofactor for TRAF2 downstream of TNF signaling required for signal transduction from TNFR1 to NF- κ B⁴³. Although TNF alone is insufficient to induce osteoclastogenesis under most conditions, it can potently synergize with low levels of RANKL to drive osteoclast generation⁴⁴, and therefore represents a major mediator of osteoclast mediated bone resorption in inflammatory disease. Thus, the S-1-P pathway may represent a particularly attractive candidate for therapeutic targeting of inflammatory osteoclasts.

Taken together, these studies have for the first time characterized at the molecular level the roles played by bone substrate in the differentiation and activation of osteoclasts. Bone regulates numerous signaling pathways, some but not all of which are dependent upon itgb3-mediated attachment to the substrate, including cell cycle progression and the generation, transport and signaling of S-1-P. Since authentic osteoclasts exist *in vivo* exclusively on bone, these findings are critical for a full understanding of osteoclast differentiation and identification of specific therapeutic targets within resorbing osteoclasts.

Methods

Differentiation of mouse BMM-derived osteoclasts on different substrates.

Devitalized mouse calvarial bone discs were prepared as described⁸. M-CSF dependent BMM were generated from bone marrow cells from 4 individual 6 week old wild-type mice (C57Bl/6) as described¹⁷. Cells were then cultured at a density of 5×10^5 per well in 24 well dishes (Corning Inc., Corning, NY) in the presence of 20 ng/ml mouse M-CSF (R&D Systems, Minneapolis, MN) or mouse M-CSF + RANKL (20 ng/ml each) (R&D Systems, Minneapolis, MN) on the devitalized bone discs, or on tissue culture plastic, or on synthetic HA (Osteologic discs, BD Bioscience, Franklin Lakes, NJ) for 1, 3 and 5 days. Following culture, RNA was extracted using Trizol, quantitated and assessed for purity, and subjected to microarray analysis. Cells in duplicate wells were fixed with cold 4% paraformaldehyde for 10 minutes for histological staining.

In a second experiment, M-CSF dependent BMM were generated from bone marrow cells from 3 wild-type mice (C57Bl/6) and 3 itgb3 deficient¹² mice as described above and cultured at a density of 5×10^5 per well in 24 well dishes (Corning Inc., Corning, NY) in the presence of mouse M-CSF + RANKL (20 ng/ml each) (R&D Systems, Minneapolis, MN) on devitalized bone discs, or on tissue culture plastic, for 5 days, prior to RNA extraction and microarray analysis or fixation and staining.

TRAP and actin ring staining. Verification of pre-osteoclasts was confirmed by staining for tartrate resistant acid phosphatase (TRAP) and actin ring formation in wild-type and itgb3 deficient osteoclasts was visualized by rhodamine-phalloidin. TRAP staining was performed using the naphthol-based method⁴⁵. Briefly, cells were incubated with 0.05 mol/L Acetate buffer, pH 5.0, containing 0.27 mmol/L naphthol AS-MX phosphate (Sigma-Aldrich, St. Louis, MO), 1% vol/vol N,N-dimethylformamide, 1.6 mmol/L Fast Red LB salt and 50 mmol/L sodium tartrate at 37°C for 10 minutes.

Following TRAP staining, cells were permeabilized with 0.1% Triton X-100 in PBS for 3–5 mins. After washing with PBS, cells were incubated with rhodamine-conjugated phalloidin solution (Molecular Probes, Carlsbad, CA) diluted 1/200 in PBS containing 1% BSA for 1 hr. Actin rings were detected by fluorescence microscopy (Olympus BX-FLA, Osaka).

Microarray experiments and data analysis. One microgram total RNA was used to synthesize cRNA using the Affymetrix expression protocol (Expression Analysis Technical Manual; Affymetrix, Santa Clara, CA). Ten micrograms labeled and fragmented cRNA was hybridized to Affymetrix MOE430.2 chips (Affymetrix, Santa Clara, CA), and detection signal was calculated using MAS5 algorithm in GCOS (Expression Analysis Technical Manual; Affymetrix) and sample normalization was performed using global scaling.

Fold change differences and p-values were calculated using ANOVA, and genes were considered differentially regulated if they had a fold change of ± 2 between groups, and if the false-discovery-rate corrected p-value was < 0.05 . Hierarchical clustering was performed with signal values on differentially-regulated genes, normalized to between 0 and 1 for each gene, and then clustered via Ward's method.

Pathway analysis was conducted by the Gene Set Enrichment Analysis (GSEA) method⁴⁶, using the detection signals as input data, and pathway sets from Biocarta.

Resulting pathways were ranked by FDR q value. Additional functional analysis was conducted on subsets of the genes using Ingenuity IPA.

Immunohistochemistry. Formalin-fixed, paraffin embedded sections from patients with inflammatory bone erosions (RA, peri-implant osteolysis) were sectioned and detected with 1 : 100 (5 µg/ml) rabbit anti-human SphK1 antibody (ab16491, abcam, Cambridge, MA) or isotype control diluted in PBS. Antigen retrieval was for 7 minutes in 10 mM EDTA pH 7.6 in a scientific microwave, followed by inhibition of endogenous hydrogen peroxidase with 3% H₂O₂ in water for 20 minutes at room temperature and blocking with: 1.5% normal goat serum (Vector Laboratories, Burlingame, CA) + 5% FCS for 30 min at room temperature. Secondary antibody and detection steps were performed using Vector Laboratories kits (Vector Laboratories, Burlingame, CA) following the manufacturers recommendations.

Sphingosine kinase inhibitors. N, N-Dimethylsphingosine [2S-(dimethylamino)-4E-octadecene-1,3R-diol; CAS Registry No: 119567-63-4] was purchased from Cayman Chemical (Ann Arbor, MI, supplied in DMSO). Compound 54 was prepared as described³⁰ and was solvated in dimethyl sulfoxide (DMSO). Inhibitors were submitted to Invitrogen/Life Technologies SelectScreen kinase profiling service for assessing selectivity against lipid kinases (lipid kinase panel) and/or protein kinases (kinome sampler panel, 50 kinases) at a concentration of 10 µmol/L. Enhanced selectivity for SphK1 versus SphK2 was confirmed for Compound 54 (100% SphK1 inhibition, with minimal inhibition of SphK2, 18% inhibition). Of protein kinases, N,N'-DMS led to 43% inhibition of TRKA and Compound 54 led to 31% inhibition of FLT3. Neither compound led to substantial inhibition of any other lipid and/or protein kinase tested (<27% inhibition; data not shown).

In vitro osteoclastogenesis assays in the presence of SphK1 inhibitors. Bone marrow macrophages (BMM) from C57BL6 mice were isolated by culture of bone marrow cells for three days on petri dishes in α-MEM medium supplemented with 10% FBS, 1% penicillin-streptomycin (Invitrogen, Carlsbad, CA) and 10% (equivalent to 140 ng/ml M-CSF) conditioned medium from the M-CSF overproducing cell line CMG⁴⁷. Adherent cells were collected by trypsinization and then cultured in multi-well tissue culture plastic dishes. For osteoclastogenesis, cells were cultured at 5×10^4 cells/ml in the same medium with GST-RANKL added to 0–50 ng/ml, in 96-well dishes (200 µl per well) or 24-well dishes (1 ml per well). Where required, slices of bovine cortical bone were inserted into the wells prior to addition of cells. Medium was changed after three days. SphK inhibitors were added at various doses for either the first 3 days, the last 2 days, or for all five days. DMSO was added at equivalent levels to control cultures. Osteoclastogenesis was assessed on day 5 by TRAP staining (Sigma-Aldrich, St. Louis, MO, kit 386A) followed by counting of TRAP-positive, multinuclear (3+ nuclei) cells. Bone resorption was assessed by removal of cells from bone slices with 2 M NaOH, and incubation for 30 minutes with 20 µg/ml peroxidase-conjugated wheat germ agglutinin (Sigma-Aldrich, St. Louis, MO) followed by 30 minutes with 3,3'-diaminobenzidine substrate solution (Vector Laboratories, Burlingame, CA). For generation of human osteoclasts, CD14-positive monocytes were prepared from PBMCs derived from de-identified normal human donors as described previously⁴⁸. Cells were then cultured at a cell density of $1-2 \times 10^6$ cells per milliliter in α-MEM medium (Invitrogen, Carlsbad, CA) supplemented with 10% fetal bovine serum (VWR, West Chester, PA) and 1% antibiotic/antimycotic (Invitrogen, Carlsbad, CA) in the presence or absence of 25 ng/ml human M-CSF (Peprotech, Rocky Hill, NJ) in 12-well tissue culture plates (1 ml per well). For osteoclastogenesis, cells were cultured at 3×10^5 cells/ml in the same medium with GST-RANKL added to 0–40 ng/ml, in 96-well dishes (200 µl per well) or 24-well dishes (1 ml per well) in the presence or absence of inhibitors. Medium was changed every three days. Osteoclastogenesis was assessed on day 7–9 by TRAP staining, as described above.

RNA extraction and qPCR. RNA was extracted (RNeasy Mini kit, QIAGEN Inc., Valencia, CA) and assessed for concentration and purity by optical density measurement. 500 ng aliquots of total cellular RNA were reverse transcribed using oligo-dT primers and MMLV reverse transcriptase (First Strand cDNA Synthesis Kit, Fermentas) as recommended by the manufacturer. Real time quantitative PCR (qPCR) was carried out in duplicate using the iCycler iQ thermal cycler detection system (Bio-Rad Laboratories Inc., Hercules, CA). Reactions included iQ™ SYBR® Green Supermix reagent (Bio-Rad Laboratories Inc., Hercules, CA), 10 ng cDNA, and forward and reverse primers each at a concentration of 250 nM in a total volume of 25 µl. mRNA amounts were normalized relative to the house-keeping genes HPRT or GAPDH, and quantified using the ΔΔCt method⁴⁹. Generation of only the correct amplification products was confirmed using melting point curve analysis of the products. The sequences of the oligonucleotide primers used were:

Mouse AnxA8: GGCTATCTGGAGCGGATTCTGGTTCGATCTT-CTCACCA

Mouse UCHL1: AGGGACAGGAAGTTAGCCCTA/AGCTTCTCCGTTTC-AGACAGA

Mouse FKBP9: AGCTTCTCCGTTTCAGACAGA/TCTGGCCGTCGAGGA-AAGT

Mouse SphK1: GATGCATGAGGTGGTGAATG/GCTACACAGGGGTTCT-GGGA

Mouse Spns2: GGCATCTTCTCTGGTCTGC/ATGATGGTGGGTGCCTA-TGGT



Mouse Cathepsin K: GAGGC GGCTATATGACCACTG/CATAACA CTTTC-
ATCCTGGCCC
Mouse HPRT: AGCTACTGTAATGATCAGTCAACG/AGAGGTCCCTTT-
CACCAGCA

1. Goldring, S. R. & Gravallese, E. M. Pathogenesis of bone erosions in rheumatoid arthritis. *Curr Opin Rheumatol* **12**, 195–199 (2000).
2. Teitelbaum, S. L. Bone resorption by osteoclasts. *Science* **289**, 1504–1508 (2000).
3. Nakashima, T., Hayashi, M. & Takayanagi, H. New insights into osteoclastogenic signaling mechanisms. *Trends Endocrinol Metab* **23**, 582–590 (2012).
4. Boyle, W. J., Simonet, W. S. & Lacey, D. L. Osteoclast differentiation and activation. *Nature* **423**, 337–342 (2003).
5. Teitelbaum, S. L. & Ross, F. P. Genetic regulation of osteoclast development and function. *Nat Rev Genet* **4**, 638–649 (2003).
6. Ishida, N. *et al.* Large scale gene expression analysis of osteoclastogenesis in vitro and elucidation of NFAT2 as a key regulator. *J Biol Chem* **277**, 41147–41156 (2002).
7. Takayanagi, H. *et al.* Induction and activation of the transcription factor NFATc1 (NFAT2) integrate RANKL signaling in terminal differentiation of osteoclasts. *Dev Cell* **3**, 889–901 (2002).
8. Crotti, T. N. *et al.* Bone matrix regulates osteoclast differentiation and annexin A8 gene expression. *J Cell Physiol* **226**, 3413–3421 (2011).
9. McHugh, K. *et al.* Annexin VIII Is a Critical Bone Matrix-dependent Osteoclast Gene Transcriptionally Regulated by RANKL and NFATc1. Paper presented at: American Society for Bone and Mineral Research 29th Annual Meeting, Honolulu, Hawaii, USA. Published by AMER SOC BONE & MINERAL RES, 2025 M ST, NW, Ste 800, Washington, DC 20036-3309 USA, DOI: 10.1002/jbm.5650221409, 2007, September 19.
10. McHugh, K. P. *et al.* Role of cell-matrix interactions in osteoclast differentiation. *Adv Exp Med Biol* **602**, 107–111 (2007).
11. McHugh, K. P. *et al.* The role of cell-substrate interaction in regulating osteoclast activation: potential implications in targeting bone loss in rheumatoid arthritis. *Ann Rheum Dis* **69 Suppl 1**, i83–85 (2010).
12. McHugh, K. P. *et al.* Mice lacking beta3 integrins are osteosclerotic because of dysfunctional osteoclasts. *J Clin Invest* **105**, 433–440 (2000).
13. Ross, F. P. & Teitelbaum, S. L. alphavbeta3 and macrophage colony-stimulating factor: partners in osteoclast biology. *Immunol Rev* **208**, 88–105 (2005).
14. Zhao, H. *et al.* Critical role of beta3 integrin in experimental postmenopausal osteoporosis. *J Bone Miner Res* **20**, 2116–2123 (2005).
15. Bakewell, S. J. *et al.* Platelet and osteoclast beta3 integrins are critical for bone metastasis. *Proc Natl Acad Sci U S A* **100**, 14205–14210 (2003).
16. Saltel, F., Destaing, O., Bard, F., Eichert, D. & Jurdic, P. Apatite-mediated actin dynamics in resorbing osteoclasts. *Mol Biol Cell* **15**, 5231–5241 (2004).
17. McHugh, K. P., Kitazawa, S., Teitelbaum, S. L. & Ross, F. P. Cloning and characterization of the murine beta(3) integrin gene promoter: identification of an interleukin-4 responsive element and regulation by STAT-6. *J Cell Biochem* **81**, 320–332 (2001).
18. Izawa, T. *et al.* c-Src links a RANK/alphavbeta3 integrin complex to the osteoclast cytoskeleton. *Mol Cell Biol* **32**, 2943–2953 (2012).
19. Morgan, E. A. *et al.* Dissection of platelet and myeloid cell defects by conditional targeting of the beta3-integrin subunit. *FASEB J* **24**, 1117–1127 (2010).
20. Nakamura, I., Duong le, T., Rodan, S. B. & Rodan, G. A. Involvement of alpha(v)beta3 integrins in osteoclast function. *J Bone Miner Metab* **25**, 337–344 (2007).
21. Nakamura, I., Lipfert, L., Rodan, G. A. & Le, T. D. Convergence of alpha(v)beta3 integrin- and macrophage colony stimulating factor-mediated signals on phospholipase Cgamma in prefusion osteoclasts. *J Cell Biol* **152**, 361–373 (2001).
22. Zhao, H., Ross, F. P. & Teitelbaum, S. L. Unoccupied alpha(v)beta3 integrin regulates osteoclast apoptosis by transmitting a positive death signal. *Mol Endocrinol* **19**, 771–780 (2005).
23. Ishii, M. *et al.* Sphingosine-1-phosphate mobilizes osteoclast precursors and regulates bone homeostasis. *Nature* **458**, 524–528 (2009).
24. Ishii, M., Kikuta, J., Shimazu, Y., Meier-Schellersheim, M. & Germain, R. N. Chemorepulsion by blood S1P regulates osteoclast precursor mobilization and bone remodeling in vivo. *J Exp Med* **207**, 2793–2798 (2010).
25. Ishii, T., Shimazu, Y., Nishiyama, I., Kikuta, J. & Ishii, M. The role of sphingosine 1-phosphate in migration of osteoclast precursors: an application of intravitral two-photon microscopy. *Mol Cells* **31**, 399–403 (2011).
26. Kikuta, J. *et al.* Sphingosine-1-phosphate-mediated osteoclast precursor monocyte migration is a critical point of control in antionbone-resorptive action of active vitamin D. *Proc Natl Acad Sci U S A* **110**, 7009–7013 (2013).
27. Pederson, L., Ruan, M., Westendorf, J. J., Khosla, S. & Oursler, M. J. Regulation of bone formation by osteoclasts involves Wnt/BMP signaling and the chemokine sphingosine-1-phosphate. *Proc Natl Acad Sci U S A* **105**, 20764–20769 (2008).
28. Ryu, J. *et al.* Sphingosine 1-phosphate as a regulator of osteoclast differentiation and osteoclast-osteoblast coupling. *EMBO J* **25**, 5840–5851 (2006).
29. Nishi, T., Kobayashi, N., Hisano, Y., Kawahara, A. & Yamaguchi, A. Molecular and physiological functions of sphingosine 1-phosphate transporters. *Biochim Biophys Acta* **1841**, 759–765 (2014).
30. Xiang, Y. *et al.* Discovery of novel sphingosine kinase-1 inhibitors. Part 2. *Bioorg Med Chem Lett* **20**, 4550–4554 (2010).
31. Aliprantis, A. O. *et al.* NFATc1 in mice represses osteoprotegerin during osteoclastogenesis and dissociates systemic osteopenia from inflammation in cherubism. *J Clin Invest* **118**, 3775–3789 (2008).
32. de la Rica, L. *et al.* PU.1 target genes undergo Tet2-coupled demethylation and DNMT3b-mediated methylation in monocyte-to-osteoclast differentiation. *Genome Biol* **14**, R99 (2013).
33. Mann, M., Barad, O., Agami, R., Geiger, B. & Hornstein, E. miRNA-based mechanism for the commitment of multipotent progenitors to a single cellular fate. *Proc Natl Acad Sci U S A* **107**, 15804–15809 (2010).
34. Miyauchi, Y. *et al.* The Blimp1-Bcl6 axis is critical to regulate osteoclast differentiation and bone homeostasis. *J Exp Med* **207**, 751–762 (2010).
35. Mizoguchi, F., Murakami, Y., Saito, T., Miyasaka, N. & Kohsaka, H. miR-31 controls osteoclast formation and bone resorption by targeting RhoA. *Arthritis Res Ther* **15**, R102 (2013).
36. Sharma, P., Patnirapong, S., Hann, S. & Hauschka, P. V. RANKL-RANK signaling regulates expression of xenotropic and polytropic virus receptor (XPR1) in osteoclasts. *Biochem Biophys Res Commun* **399**, 129–132 (2010).
37. Wang, Y., Inger, M., Jiang, H., Tenenbaum, H. & Glogauer, M. CD109 plays a role in osteoclastogenesis. *PLoS One* **8**, e61213 (2013).
38. Ogasawara, T. *et al.* Osteoclast differentiation by RANKL requires NF-kappaB-mediated downregulation of cyclin-dependent kinase 6 (Cdk6). *J Bone Miner Res* **19**, 1128–1136 (2004).
39. Rimondi, E., Zweyer, M., Ricci, E., Fadda, R. & Secchiero, P. Receptor activator of nuclear factor kappa B ligand (RANKL) modulates the expression of genes involved in apoptosis and cell cycle in human osteoclasts. *Anat Rec (Hoboken)* **290**, 838–845 (2007).
40. Sankar, U., Patel, K., Rosol, T. J. & Ostrowski, M. C. RANKL coordinates cell cycle withdrawal and differentiation in osteoclasts through the cyclin-dependent kinase inhibitors p27KIP1 and p21CIP1. *J Bone Miner Res* **19**, 1339–1348 (2004).
41. Kim, H. J. *et al.* Suppression of osteoclastogenesis by N,N-dimethyl-D-erythro-sphingosine: a sphingosine kinase inhibition-independent action. *Mol Pharmacol* **72**, 418–428 (2007).
42. Baker, D. A., Barth, J., Chang, R., Obeid, L. M. & Gilkeson, G. S. Genetic sphingosine kinase 1 deficiency significantly decreases synovial inflammation and joint erosions in murine TNF-alpha-induced arthritis. *J Immunol* **185**, 2570–2579 (2010).
43. Alvarez, S. E. *et al.* Sphingosine-1-phosphate is a missing cofactor for the E3 ubiquitin ligase TRAF2. *Nature* **465**, 1084–1088 (2010).
44. Lam, J. T. S., Barker, J. E., Kanagawa, O., Ross, F. P. & Teitelbaum, S. L. TNF-alpha induces osteoclastogenesis by direct stimulation of macrophages exposed to permissive levels of RANK ligand. *J Clin Invest* **106**, 1481–1488 (2000).
45. Burstone, M. S. Histochemical demonstration of acid phosphatases with naphthol AS-phosphates. *J Natl Cancer Inst* **21**, 523–539 (1958).
46. Subramanian, A. *et al.* Gene set enrichment analysis: a knowledge-based approach for interpreting genome-wide expression profiles. *Proc Natl Acad Sci U S A* **102**, 15545–15550 (2005).
47. Takeshita, S., Kaji, K. & Kudo, A. Identification and characterization of the new osteoclast progenitor with macrophage phenotypes being able to differentiate into mature osteoclasts. *J Bone Miner Res* **15**, 1477–1488 (2000).
48. Rakshit, D. S. *et al.* Wear Debris Inhibition of Anti-Osteoclastogenic Signaling by Interleukin-6 and Interferon-[gamma] Mechanistic Insights and Implications for Periprosthetic Osteolysis. *J Bone Joint Surg Am* **88**, 788–799 (2006).
49. Livak, K. J. & Schmittgen, T. D. Analysis of relative gene expression data using real-time quantitative PCR and the 2(-Delta Delta C(T)) Method. *Methods* **25**, 402–408 (2001).

Acknowledgments

TC was funded by an American Arthritis Fellowship. We would like to thank Dr. Steven Brunette for providing SphK1 inhibitor and helpful discussions on inhibitor properties.

Author contributions

E.P. helped conceive the study, performed the inhibitor cell culture and qPCR studies and wrote the manuscript. T.C. performed the isolation and culture of cells on different substrates and the actin ring staining experiments as well as RNA isolation and manuscript feedback. Z.S. performed the immunohistochemistry experiments. J.S. helped conceive the in vitro inhibitor studies, co-ordinated inhibitor acquisition and characterization and provided input in writing the manuscript. J.L., J.H., A.H. and J.D. performed the microarray experiments and analysis of expression profiles and pathways analysis. G.N. and S.R.G. helped conceive the study and write the manuscript. K.M. helped conceive the study and perform the cell culture experiments and RNA extraction of osteoclasts on different substrates, and wrote the manuscript.

Additional information

Competing financial interests: The authors declare no competing financial interests.

How to cite this article: Purdue, P.E. *et al.* Comprehensive profiling analysis of actively resorbing osteoclasts identifies critical signaling pathways regulated by bone substrate. *Sci. Rep.* **4**, 7595; DOI:10.1038/srep07595 (2014).



This work is licensed under a Creative Commons Attribution-NonCommercial-NoDerivs 4.0 International License. The images or other third party material in this article are included in the article's Creative Commons license, unless indicated otherwise in the credit line; if the material is not included under the Creative

Commons license, users will need to obtain permission from the license holder in order to reproduce the material. To view a copy of this license, visit <http://creativecommons.org/licenses/by-nc-nd/4.0/>